Commun. Comput. Phys.
doi: 10.4208/cicp.210815.180316a

Vol. **20**, No. 5, pp. 1163-1182
November 2016

Reinitialization of the Level-Set Function in 3d Simulation of Moving Contact Lines

Shixin Xu[1] and Weiqing Ren[1,2,*]

[1] *Department of Mathematics, National University of Singapore, 119076, Singapore.*
[2] *Institute of High Performance Computing, Agency for Science, Technology and Research, 138632, Singapore.*

Received 21 August 2015; Accepted (in revised version) 18 March 2016

Abstract. The level set method is one of the most successful methods for the simulation of multi-phase flows. To keep the level set function close the signed distance function, the level set function is constantly reinitialized by solving a Hamilton-Jacobi type of equation during the simulation. When the fluid interface intersects with a solid wall, a moving contact line forms and the reinitialization of the level set function requires a boundary condition in certain regions on the wall. In this work, we propose to use the dynamic contact angle, which is extended from the contact line, as the boundary condition for the reinitialization of the level set function. The reinitialization equation and the equation for the normal extension of the dynamic contact angle form a coupled system and are solved simultaneously. The extension equation is solved on the wall and it provides the boundary condition for the reinitialization equation; the level set function provides the directions along which the contact angle is extended from the contact line. The coupled system is solved using the 3rd order TVD Runge-Kutta method and the Godunov scheme. The Godunov scheme automatically identifies the regions where the angle condition needs to be imposed. The numerical method is illustrated by examples in three dimensions.

AMS subject classifications: 65Z05, 76T10

Key words: Level set method, two-phase flows, moving contact lines, contact angle, reinitialization, level set function.

1 Introduction

Contact line refers to the line where a fluid interface intersects with a solid wall. The modeling and simulation of moving contact lines have attracted much attention in recent years. This is not only due to the many industrial applications, e.g. in microfluidics, but

*Corresponding author. *Email addresses:* matxs@nus.edu.sg (S. Xu), matrw@nus.edu.sg (W. Ren)

 ©2016 Global-Science Press

https://doi.org/10.4208/cicp.210815.180316a Published online by Cambridge University Press

also scientific interests such as the stress singularity, contact angle hysteresis, etc.. We refer to the review articles [1–4] and the monographs [5–7] for discussions of the current status of the moving contact lines problem.

Some numerical methods have been developed for the simulation of multi-phase flows with moving contact lines. These include the volume of fluids method [8–10], the front tracking method [11, 12], the phase field method [13–16], the level set method [17–20], etc.. More can be found in a recent review paper [21]. In this paper, we will focus on the level set method, in particular, the boundary condition for the reinitialization of the level set function in the simulation of the moving contact lines in three dimensions (3d).

In the level set method, the interface is implicitly represented using the zero-level set of a function $\phi(\mathbf{x})$, which is called the level set function. Usually the signed distance function is used as the level set function. It is evolved according to the velocity field of the fluids $\mathbf{u}$,

$$\frac{\partial \phi}{\partial t} + \mathbf{u} \cdot \nabla \phi = 0. \tag{1.1}$$

During the evolution, the level set function is usually distorted in the sense that it deviates from the signed distance function and develops large variations. This may affect the accuracy of the numerical solution. To prevent this from happening, the level set function is reinitialized during the evolution. This is done by solving the following reinitialization equation in pseudo time τ [22]:

$$\frac{\partial \phi}{\partial \tau} + S(\phi_0)(|\nabla \phi| - 1) = 0, \tag{1.2}$$

where ϕ_0 is the level set function before the reinitialization, and $S(\cdot)$ is the sign function. Eq. (1.2) is a transport equation with the velocity

$$\mathbf{v}_\phi = S(\phi_0)\mathbf{n}, \quad \text{where} \quad \mathbf{n} = \frac{\nabla \phi}{|\nabla \phi|}. \tag{1.3}$$

Denote the outward unit normal of the wall by $\mathbf{n}_w$, then it is readily seen that Eq. (1.2) needs a boundary condition in regions where $\mathbf{v}_\phi \cdot \mathbf{n}_w < 0$ (i.e. when the transport velocity points into the fluid domain) on the wall; in contrast, no boundary condition can be imposed in regions where $\mathbf{v}_\phi \cdot \mathbf{n}_w > 0$. This is illustrated in Fig. 1, where the fluid interface is indicated by the bold curve. To reinitialize the given level set function shown in the figure, a boundary condition is needed on the wall outside the droplet, whereas no boundary condition is needed inside the droplet. After solving the reinitialization equation, the level set function becomes the signed distance function to the interface, except in the wedge (shaded region) where the level set function depends on the boundary condition specified on the wall.

Several strategies have been proposed regarding the boundary condition for the reinitialization equation. Most of these methods are for 2d problems as shown in Fig. 1, in

https://doi.org/10.4208/cicp.210815.180316a Published online by Cambridge University Press

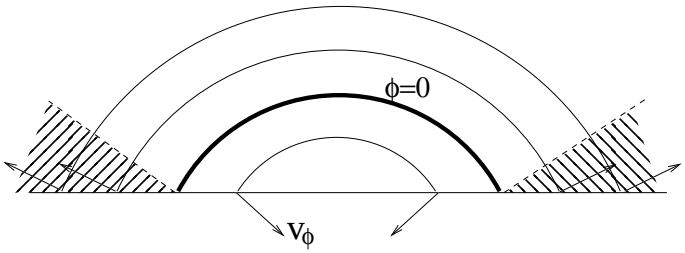


Figure 1: Schematics of the level set function ϕ. The zero-level set of ϕ, which represents the fluid interface, is indicated by the bold line. The arrows are the transport velocity $\mathbf{v}_\phi$ in the reinitialization equation. A boundary condition is needed on the wall where $\mathbf{v}_\phi$ points from the wall into the fluid domain. After reinitialization, the level set function in the shaded region depends on the boundary condition specified on the wall.

which the contact line reduces to two contact points. In Ref. [17], the contact point is first located and the fluid interface is extended into the wall at the contact point by a linear extrapolation. Several layers of ghost points are introduced next to the wall; on these ghost points, the level set function is defined either by the distance to the extended interface, or the linear extrapolation of the level set function. This type of methods requires the extension of the fluid interface, which is not straightforward for 3d problems. In Ref. [23], the grid points on the wall where a boundary condition is needed are first identified, then the level set function on these points are obtained by solving the following relaxation equation:

$$\frac{\partial \phi}{\partial \tau} = \cos\theta - \cos\theta_0, \tag{1.4}$$

where θ is the angle between the iso-surfaces of ϕ and the wall, i.e. $\cos\theta = -\nabla\phi\cdot\mathbf{n}_w/|\nabla\phi|$, and θ_0 is the angle before reinitialization. This equation aims at keeping the angle of the isosurfaces of ϕ to be the same as that prescribed in the initial data ϕ_0. This requires a proper choice of the initial data. In Refs. [19, 24–26], the contact angle was used as the boundary condition, and different numerical schemes were proposed to impose this angle condition. In all these work, the system (a droplet) was assumed to be axisymmetric, thus the contact angle is constant along the contact line. In these work, this spatially uniform contact angle was imposed on the level set function along the wall during reinitialization.

In the current work, we consider general 3d problems in which the dynamic contact angle may vary along the contact line. This is the case, for example, when a droplet slides down a tilted plane in which the dynamic contact angle in the front (i.e. the advancing contact angle) differs from that in the back (i.e. the receding contact angle), though the equilibrium contact angle may be the same everywhere on the wall, or when a droplet spreads on a chemically heterogeneous surface in which the contact angle is position dependent.

Similar to the earlier work, we also propose to impose the angle condition on the level set function when solving the reinitialization equation. However, in the 3d problems

https://doi.org/10.4208/cicp.210815.180316a Published online by Cambridge University Press

considered in this work, due to the variation of the dynamic contact angle along the contact line, the angle away from the contact line needs to be carefully specified so that it is consistent with the angle along the contact line. This is in contrast to the 2d or axisymmetric systems considered in the earlier work, where a spatially constant angle was used everywhere on the wall.

In our method, the angle on the wall is obtained from the normal extension of the dynamic contact angle from the contact line. The reinitialization equation for the level set function and the extension equation for the angle form a coupled system and are solved at the same time. The later is solved on the wall and it provides the boundary condition for the level set function; the level set function provides the directions along which the contact angle is extended.

The paper is organized as follows. In Section 2, we describe the coupled equations and propose numerical methods for these equations. The upwind scheme in the numerical method automatically identifies the regions where the angle condition needs to be imposed. In Section 3, we present numerical examples to illustrate the performance of the proposed method. The paper is concluded in Section 4.

2 The numerical method

As shown in Fig. 2, we consider an evolving droplet on a solid wall in the three-dimensional space. The surface of the droplet intersects with the solid wall at the contact line. We denote the computational domain containing the droplet by Ω. The lower boundary of Ω lies on the solid wall and is denoted by $\partial\Omega_w$. We use the Cartesian coordinate so that the solid wall is on the plane $z=0$. In this work, we will focus on the contact line and the boundary condition on the solid wall, therefore we simply assume the periodic boundary condition in the x and y directions.

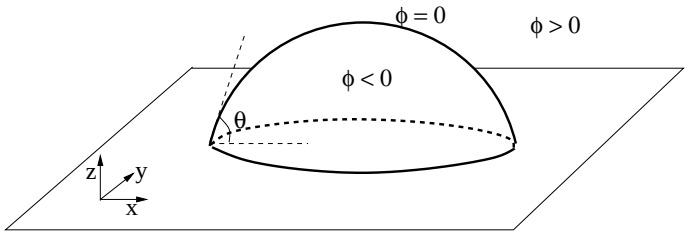


Figure 2: Schematics of a droplet on a solid wall. The closed curve at which the fluid interface intersects with the wall is the contact line. θ denotes the contact angle, and ϕ is the level set function.

Equations. To solve the reinitialization equation (1.2) for a given interface, one needs to specify a boundary condition for the level set function ϕ in the region where $S(\phi)\partial_z\phi > 0$ on the solid wall. We denote this region by $\partial\Omega_{w,c}$. Here we require the angle θ at which the iso-surface of ϕ intersects with the wall equals to some specified value. In principle,

https://doi.org/10.4208/cicp.210815.180316a Published online by Cambridge University Press

we are free to use any value for θ as long as it is consistent with the dynamic contact angle of the fluid interface. The simplest method, which guarantees the consistency, is to use the normal extension of the dynamic contact angle from the contact line. Note that for an evolving interface, the dynamic contact angle depends on the local contact line velocity; therefore, in general it differs from the equilibrium contact angle given by the Young's relation and varies along the contact line.

The extension of the contact angle is done by solving the normal extension equation on the wall [27–29]

$$\frac{\partial\theta}{\partial\tau}+S(\phi)\mathbf{n}_s(\phi)\cdot\nabla_s\theta=0,\quad \text{for } (x,y)\in\partial\Omega_w, \tag{2.1}$$

where $\mathbf{n}_s=\nabla_s\phi/|\nabla_s\phi|$ and $\nabla_s=(\partial_x,\partial_y)$ is the surface gradient on the wall. In this equation, the contact angle of the fluid interface at the contact line is extended to the wall following the normal direction of the level curves of ϕ on the wall. This extended angle is used as the boundary condition for the reinitialization equation.

The extension equation (2.1) and the reinitialization equation (1.2) form a coupled system: The extension equation provides the boundary condition for the reinitialization equation, while the latter provides the directions along which the angle is extended. Thus, we solve these two equations concurrently:

$$\frac{\partial\phi}{\partial\tau}+S(\phi_0)(|\nabla\phi|-1)=0,\quad \mathbf{x}\in\Omega, \tag{2.2a}$$

$$\lambda\frac{\partial\theta}{\partial\tau}+S(\phi)\mathbf{n}_s(\phi)\cdot\nabla_s\theta=0,\quad \mathbf{x}\in\partial\Omega_w. \tag{2.2b}$$

Eq. (2.2a) is supplemented with the boundary condition

$$\partial_z\phi=\sqrt{(\partial_x\phi)^2+(\partial_y\phi)^2}\cot\theta,\quad \mathbf{x}\in\partial\Omega_{w,c}. \tag{2.3}$$

The parameter λ in Eq. (2.2b) is to control the propagation speed of θ relative to the dynamics of ϕ. A small λ increases the propagation speed of θ. In particular, in the limit $\lambda\to 0$, at any instant the angle on the wall equals to the contact angle extended from the contact line according to the current configuration of ϕ. On the other hand, a larger λ decreases the extension speed. In this work we use $\lambda=1$.

The above equations are solved with the initial condition

$$\phi(\mathbf{x},0)=\phi_0(\mathbf{x}),\quad \mathbf{x}\in\Omega. \tag{2.4}$$

The initial value of θ is obtained from ϕ_0:

$$\theta(\mathbf{x},0)=\arccos\left(\partial_z\phi/|\nabla\phi|\right),\quad \mathbf{x}\in\partial\Omega_w. \tag{2.5}$$

Remark 2.1. In Eq. (2.2b), the contact angle is extended to the whole boundary $\partial\Omega_w$. However, when solving the reinitialization equation, it is imposed as the boundary condition for ϕ only in the region $\partial\Omega_{w,c}$. This is achieved by using an upwinding scheme to be discussed next in the numerical discretization.

https://doi.org/10.4208/cicp.210815.180316a Published online by Cambridge University Press

To better conserve the droplet volume, a constrained reinitialization technique (HCR2) proposed by Hartmann *et al.* [30] is used in this work. In this scheme, a delta force, which concentrates on the fluid interface, is added to Eq. (2.2a). This delta force is to keep the interface pinned in space during the reinitialization process. We refer to Ref. [30] for details of this technique.

Spatial discretization. The coupled equations in (2.2), (2.3) are solved using the finite difference method on a uniform mesh. We use equal mesh size in the three directions, and denote the grid points by (x_i,y_j,z_k) where the integers i,j and k range from 0 to N_x, N_y and N_z respectively. The zero-th level of the mesh in the z direction i.e. $\{(x_i,y_j,z_0)\}$, defines a uniform mesh for the 2d domain $\partial\Omega_w$. We denote by $\phi^m_{i,j,k}$ the numerical solution of ϕ at the grid point (x_i,y_j,z_k) and the time $\tau_m=m\Delta\tau$, where $\Delta\tau$ is the time step; similarly, we denote by $\theta^m_{i,j}$ the numerical solution of θ at the grid point (x_i,y_j,z_0) and the time τ_m.

In Eq. (2.2a), the derivatives in $|\nabla\phi|=\left((\partial_x\phi)^2+(\partial_y\phi)^2+(\partial_z\phi)^2\right)^{1/2}$ are approximated using the Godunov scheme [31]; for example,

$$(\partial_x\phi)^2\approx(D_x\phi)^2=\begin{cases}\max\left(|a^+|^2,|b^-|^2\right), & \text{if } S(\phi)\le 0,\\ \max\left(|a^-|^2,|b^+|^2\right), & \text{if } S(\phi)>0,\end{cases} \tag{2.6}$$

where

$$a^+=\max\left(D^+_x\phi,0\right),\quad a^-=\min\left(D^+_x\phi,0\right), \tag{2.7a}$$
$$b^+=\max\left(D^-_x\phi,0\right),\quad b^-=\min\left(D^-_x\phi,0\right). \tag{2.7b}$$

The one-sided differences $D^+_x\phi$ and $D^-_x\phi$ are computed using the third-order WENO scheme [31]:

$$\left(D^+_x\phi\right)_{i,j,k}=\frac{(1-\omega_+)}{2h}\left(\phi_{i+1,j,k}-\phi_{i-1,j,k}\right)+\frac{\omega_+}{2h}\left(-3\phi_{i,j,k}+4\phi_{i+1,j,k}-\phi_{i+2,j,k}\right),$$
$$\left(D^-_x\phi\right)_{i,j,k}=\frac{(1-\omega_-)}{2h}\left(\phi_{i+1,j,k}-\phi_{i-1,j,k}\right)+\frac{\omega_-}{2h}\left(3\phi_{i,j,k}-4\phi_{i-1,j,k}+\phi_{i-2,j,k}\right),$$

where

$$\omega_+=\frac{1}{1+2r_+^2},\quad \omega_-=\frac{1}{1+2r_-^2},$$
$$r_+=\frac{\eta+(\phi_{i+2,j,k}-2\phi_{i+1,j,k}+\phi_{i,j,k})}{\eta+(\phi_{i,j,k+1}-2\phi_{i,j,k}+\phi_{i-1,j,k})},$$
$$r_-=\frac{\eta+(\phi_{i,j,k}-2\phi_{i-1,j,k}+\phi_{i-2,j,k})}{\eta+(\phi_{i,j,k+1}-2\phi_{i,j,k}+\phi_{i-1,j,k})},$$

and η is a small parameter. Similar schemes are used to approximate ϕ_y and ϕ_z.

https://doi.org/10.4208/cicp.210815.180316a Published online by Cambridge University Press

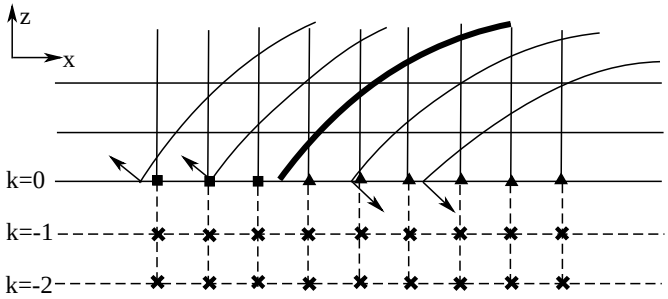


Figure 3: Schematics of the computational mesh in 2d. The bold curve is the interface. The line indicated by $k=0$ is the solid wall. The points indicated by crosses ($\times$) are the ghost points. The z-derivative of ϕ on the points indicated by squares (■) and triangles (▲) are computed using $D_z^-\phi$ and $D_z^+\phi$, respectively.

The discretization of ϕ_z on the solid wall $\partial\Omega_w$ requires the values of ϕ at the ghost points (x_i,y_j,z_{-1}) and (x_i,y_j,z_{-2}); these values are defined according to the current value $\theta_{i,j}$ obtained by solving (2.2a):

$$\phi_{i,j,-k}=\phi_{i,j,0}-kh\sqrt{(D_x\phi)^2_{i,j,0}+(D_y\phi)^2_{i,j,0}}\cot\theta_{i,j},\quad k=1,2. \tag{2.8}$$

This extrapolation, together with the Godunov scheme (2.6), makes the angle condition be imposed only in regions where it is needed. This is illustrated in Fig. 3. Without loss of generality, we assume the interface has an acute contact angle. In this case, the boundary condition is only needed in the region to the left of the contact line, and this is the region we denoted by $\partial\Omega_{w,c}$ earlier. On the solid wall, the one-sided differences $D_z^\pm\phi$ are both positive (at least near the contact line where the reinitialization equation is solved in the local level set method to be discussed below). Then according to (2.6), $D_z^-\phi$ (thus the angle θ) is used in the region to the left of the contact line where $S(\phi)>0$; in contrast, $D_z^+\phi$ is used in the region to the right of the contact line where $S(\phi)<0$. Since the angle θ has little effect on $D_z^+\phi$, the angle condition is not imposed in the region to the right of the contact line.

The extension equation for θ is solved in the 2d domain $\partial\Omega_w$ on the wall. Derivatives in the unit vector $\mathbf{n}_s=\nabla_s\phi/|\nabla_s\phi|$ are computed using upwind finite difference [22]; for example, $\partial_x\phi$ is computed using

$$\mathcal{D}_x\phi_{i,j,0}=\begin{cases}\phi_{i,j,0}-\phi_{i-1,j,0}, & \text{if } \phi_{i-1,j,0}\le\min\{\phi_{i,j,0},\phi_{i+1,j,0}\},\\ \phi_{i+1,j,0}-\phi_{i,j,0}, & \text{if } \phi_{i+1,j,0}\le\min\{\phi_{i,j,0},\phi_{i-1,j,0}\},\\ 0, & \text{if } \phi_{i,j,0}\le\min\{\phi_{i-1,j,0},\phi_{i+1,j,0}\},\end{cases} \tag{2.9}$$

and similarly for $\partial_y\phi$. The derivatives in $\nabla_s\theta$ are computed by the third-order WENO scheme.

The Local level set method. Since the level set function is only needed near the interface, we employ the local level set technique [32, 33] to improve the efficiency. The

https://doi.org/10.4208/cicp.210815.180316a Published online by Cambridge University Press

reinitialization and extension equations in (2.2) are only solved near the interface. Specifically, the level set function and the angle θ are only computed within the tube defined by

$$\mathcal{T}^m = \left\{ (x_i, y_j, z_k) : \min_{a,b,c=-1,0,1} |\phi^m_{i+a,j+b,k+c}| < \gamma \right\}. \tag{2.10}$$

For given ϕ^m, the reinitialization equation is solved in $\mathcal{T}^m$ by one time step, and the solution is denoted by $\phi^{m,*}$. The new level set function is then defined as

$$\phi^{m+1} = \begin{cases} -\gamma, & \text{if } \phi^{m,*} < -\gamma, \\ \phi^{m,*}, & \text{if } |\phi^{m,*}| \le \gamma, \\ \gamma, & \text{if } \phi^{m,*} > \gamma. \end{cases} \tag{2.11}$$

Since the reinitialization equation is not solved outside the tube, there is no need to define the angle θ outside the tube.

Finally, the spatially discretized equations are integrated in time using the third-order TVD Runge-Kutta method [34].

The major steps of the numerical method are summarized as follows. Let ϕ^m and θ^m be the solution at the m-th time step, the computation of the solutions at the new time step proceeds as follows:

Step 1. Solve Eq. (2.2b) for θ^{m+1} on the wall and inside $\mathcal{T}^m$, using ϕ^m;

Step 2. Extend ϕ^m to the ghost points below the wall using θ^{m+1};

Step 3. Solve Eq. (2.2a) for ϕ^{m+1} inside the tube $\mathcal{T}^m$.

The performance of the numerical method is illustrated using examples in the next section.

3 Numerical examples

In this section, we illustrate the performance of the proposed reinitialization method using some representative examples in 3d. We first test the numerical method for fixed interfaces (Example 1), then we consider the situation in which the interface is advected by a given velocity field (Example 2); finally the reinitialization of the level set function is coupled with the Navier-Stokes equation (Examples 3 and 4). In all the simulations, we take $\gamma = 15h$, $\Delta\tau = h/10$, and use periodic boundary condition in x and y directions. Unless otherwise specified, the grid size is set as $h = 1/80$.

https://doi.org/10.4208/cicp.210815.180316a Published online by Cambridge University Press

Example 1. In this example, we solve the reinitialization equation for a given interface. First we consider an interface in the shape of a spherical cap. The interface is given by the zero level set of

$$f_0(\mathbf{x}) = |\mathbf{x}-\mathbf{x}_0| - 0.5, \tag{3.1}$$

where the center $\mathbf{x}_0 = (0.75, 0.75, -0.25\sqrt{3})$ and $|\cdot|$ denotes the Euclidean norm. The interface intersects with the wall at $z=0$ at the contact angle 30°. The initial condition for the level set function is taken as $\phi_0 = \alpha f_0(\mathbf{x})$. Note that $|\nabla\phi_0| = |\alpha|$, so the parameter α controls the deviation of ϕ_0 from the signed distance function. The computational domain is $[0,1.5]^2 \times [0,0.5]$. The numerical results obtained using the initial condition with $\alpha = 2$ are shown in Fig. 4. We also solved the reinitialization equation with $\alpha = 0.5$, and obtained the same results.

The reinitialized level set function $\phi(\mathbf{x})$ is compared with $f_0(\mathbf{x})$ in Fig. 4(a). The function $f_0(\mathbf{x})$ is the signed distance function to the sphere $|\mathbf{x}-\mathbf{x}_0| = 0.5$ in the whole space R^3. It is seen that ϕ agrees well with $f_0(\mathbf{x})$ except in the wedge between the wall and the line perpendicular to the interface (bold line). Inside this wedge, the reinitialized level set function depends on the boundary condition imposed on the wall. As seen from Fig. 4(a),

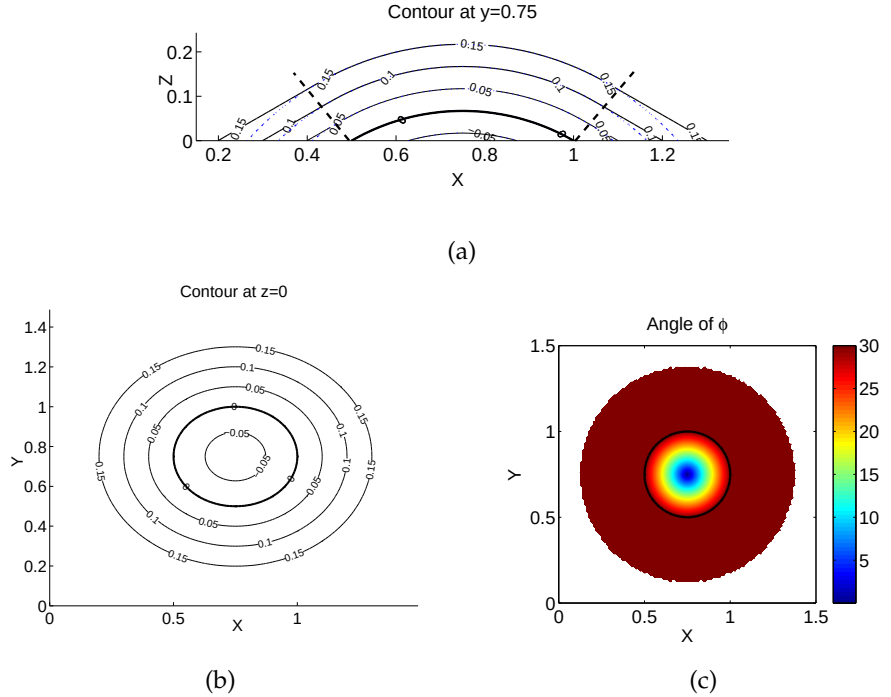


Figure 4: The reinitialized level set function for a given interface with contact angle 30° (Example 1). (a): Contour of the reinitialized level set function at $y=0.75$ (solid line). The bold line is the interface. The dashed lines are the contour of $f_0(\mathbf{x})$ in Eq. (3.1). (b): Contour of the reinitialized level set function at $z=0$. (c): The angle that the isosurfaces of ϕ make with the wall. The bold line is the contact line.

https://doi.org/10.4208/cicp.210815.180316a Published online by Cambridge University Press

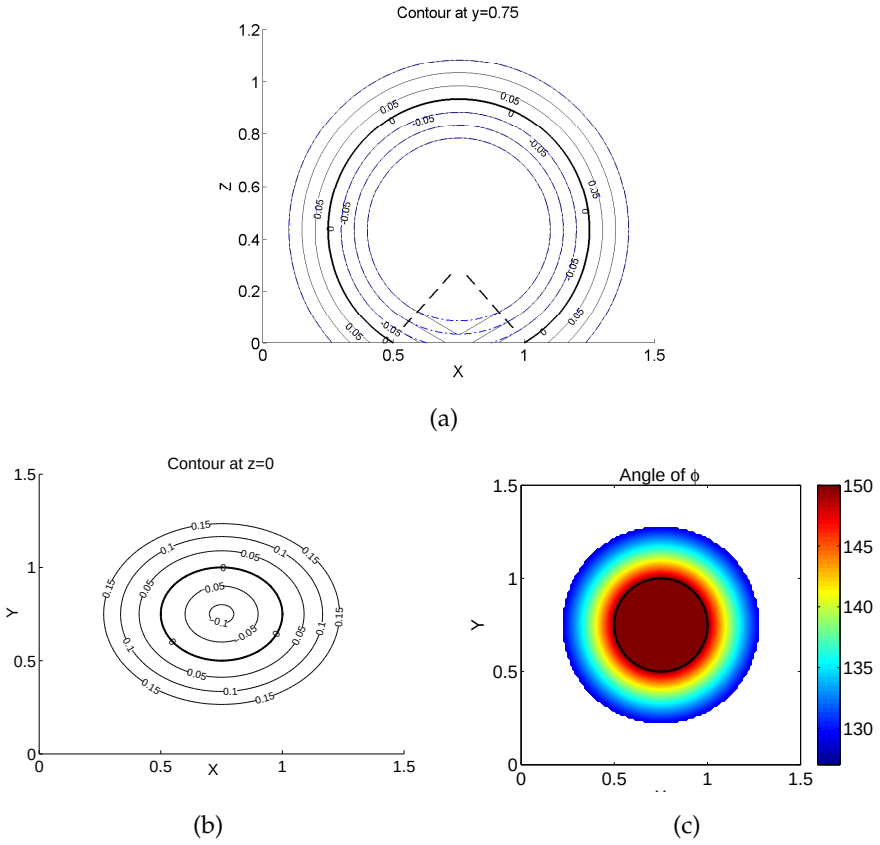


Figure 5: The reinitialized level set function for a given interface with contact angle 150° (Example 1). (a): Contour of the reinitialized level set function at $y=0.75$ (solid line). The bold line is the interface. The dashed line is the contour of $f_1(\mathbf{x})$ in Eq. (3.2). (b): Contour of the reinitialized level set function at $z=0$. (c): The angle that the isosurfaces of ϕ make with the wall. The bold line is the contact line.

the cross sections of the iso-surfaces of ϕ are straight lines which intersect with the wall at the angle $\theta=30^\circ$.

The angle θ obtained by solving the extension equation equals to 30° on the wall; however this extended angle is only imposed on the level set function outside the droplet. Inside the droplet, no boundary condition is needed and the extended angle θ is not used when solving the reinitialization equation. In Fig. 4(c), we show the angle that the isosurfaces of ϕ make with the wall. It can be seen that this angle differs from the extended angle θ inside the droplet.

The numerical method works equally well for interfaces with large contact angle. We solved the reinitialization equation for the interface given by the zero level set of

$$f_1(\mathbf{x})=|\mathbf{x}-\mathbf{x}_1|-0.5, \tag{3.2}$$

where the center $\mathbf{x}_1=(0.75,0.75,0.25\sqrt{3})$. The wall is at $z=0$ so the contact angle of the interface is 150°. The computational domain is $[0,1.5]^3$. The numerical results for ϕ

https://doi.org/10.4208/cicp.210815.180316a Published online by Cambridge University Press

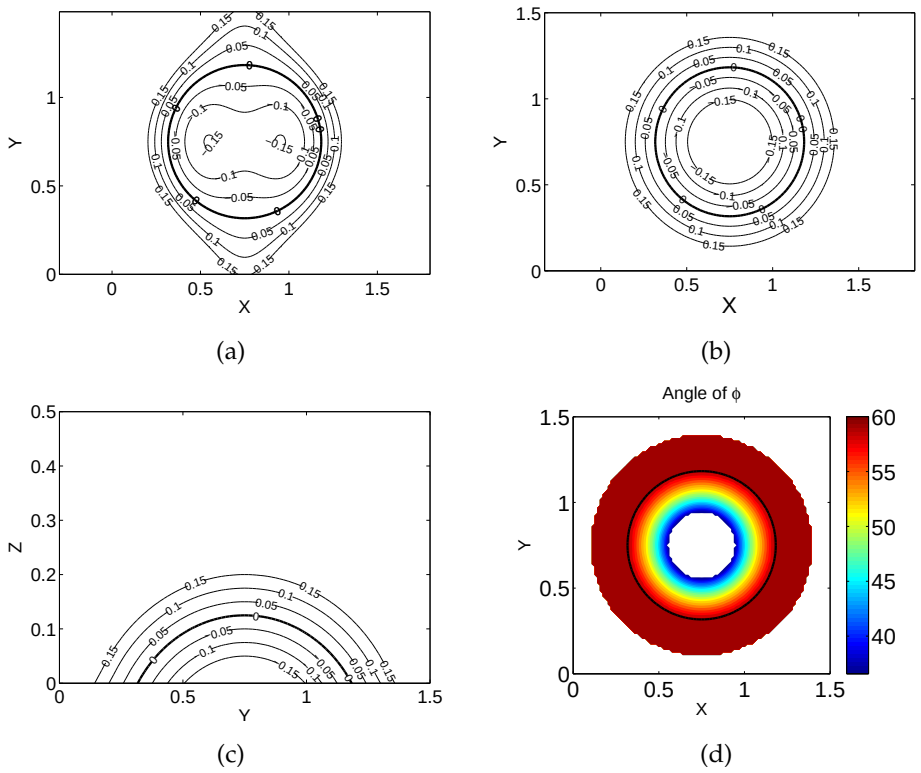


Figure 6: The reinitialized level set function from a distorted initial function (Example 1). (a): Contour of the initial level set function ϕ_0 at $z=0$. (b)-(c): Contour of the reinitialized level set function ϕ at $z=0$ and $x=0.75$, respectively. (d): The angle that the isosurfaces of ϕ make with the wall. The bold line is the contact line.

computed using the initial value $\phi_0 = 2f_1(x)$ are shown in Fig. 5. In this example, the extended angle θ equals to 150° on the wall; it is used as the boundary condition for ϕ in the region enclosed by the contact line, so the isosurfaces of the reinitialized level set function makes the angle 150° with the wall inside the droplet. Outside the droplet, no boundary condition is needed, and the reinitialized level set function agrees with the signed distance function $f_1(\mathbf{x})$ as shown in Fig. 5(a).

Finally, we consider the case where the initial level set function is largely distorted from the signed distance function. The initial value of ϕ is given by

$$\phi_0(\mathbf{x}) = (1+0.5\sin(2\pi x))\,(|\mathbf{x}-\mathbf{x}_2|-0.5), \tag{3.3}$$

where $\mathbf{x}_2 = (0.75, 0.75, -0.25)$. The wall is at $z=0$ so the contact angle of the interface $|\mathbf{x}-\mathbf{x}_2|=0.5$ is 60°. The computational domain is $[0,1.5]^2\times[0,0.5]$. The contour of ϕ_0 at $z=0$ is shown in Fig. 6(a). Cross-sections of the level set function after the reinitialization are shown in panels (b) and (c) in Fig. 6. The angle at the wall computed from the reinitialized level set function is shown in Fig. 6(d). This example shows our method can handle cases when the initial level set function is not well-prepared.

https://doi.org/10.4208/cicp.210815.180316a Published online by Cambridge University Press

Example 2. In this example, the interface evolves under a given shear flow. The initial level set function is given by $\phi_0 = |\mathbf{x}-\mathbf{x}_3|-0.5$, where $\mathbf{x}_3 = (0.75,0.75,0)$, so the initial interface is a semi-sphere centered at $\mathbf{x}_3$ with radius 0.5. The level set function is evolved according to

$$\phi_t + \mathbf{u}\cdot\nabla\phi = 0, \tag{3.4}$$

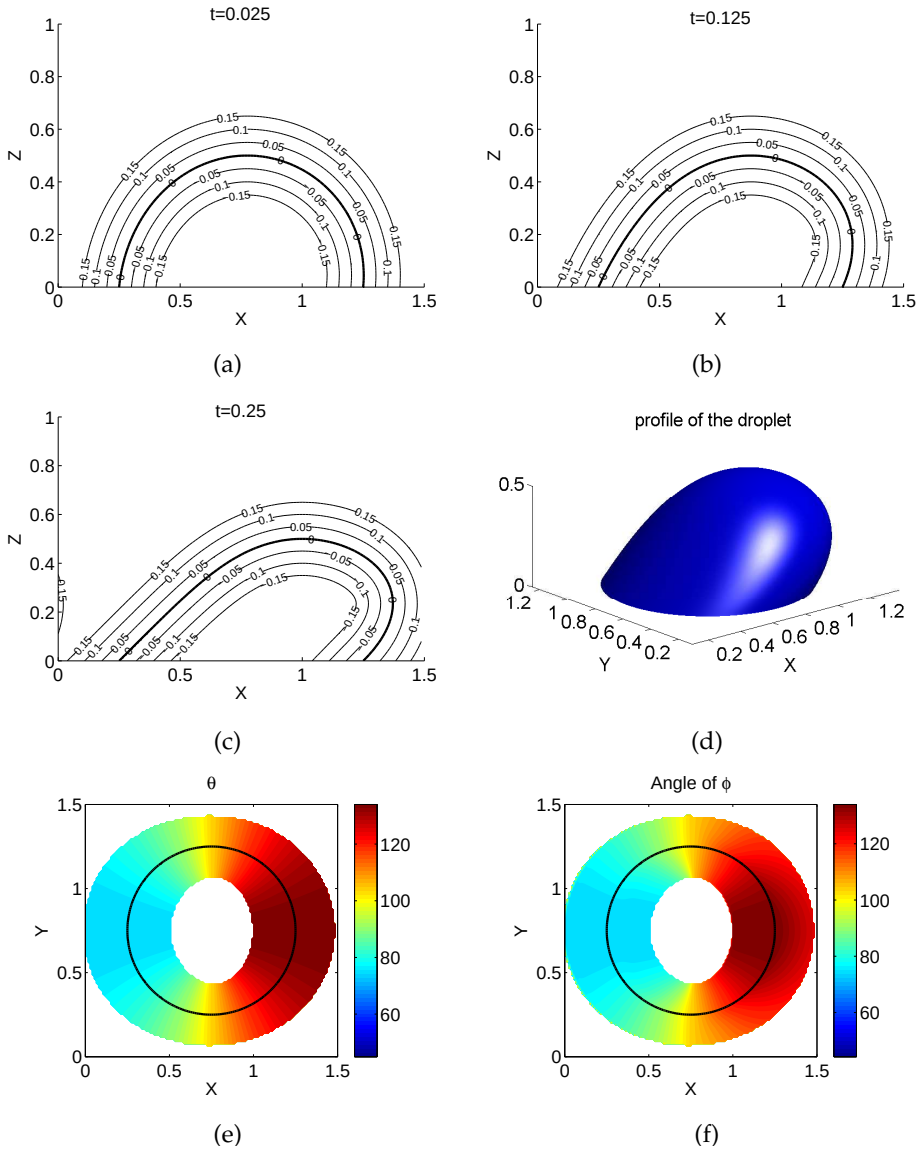


Figure 7: An evolving droplet under the shear flow $\mathbf{u} = (4z(1-z),0,0)$. (a)-(c): Contours of the level set function at $y = 0.75$ and $t = 0.025$, 0.125, 0.25 respectively. (d): Configuration of the droplet at $t = 0.25$. (e): The extended angle θ at $t = 0.25$. (f): The angle that the isosurfaces of ϕ make with the wall at $t = 0.25$.

https://doi.org/10.4208/cicp.210815.180316a Published online by Cambridge University Press

where the velocity field $\mathbf{u}=(4z(1-z),0,0)$. The computational domain is $[0,1.5]^2\times[0,1]$. The above equation is solved using the third-order TVD Runge-Kutta method with time step $\Delta t=h/5$.

The level set function is reinitialized at each time step, by solving the equations in (2.2) for 200 steps in τ. The numerical results are shown in Fig. 7. The first three panels (a)-(c) show the cross sections of ϕ at three different times. In panel (d), we plot the instantaneous interface profile at $t=0.25$. The angle θ extended from the contact line and the angle computed from the level set function at $t=0.25$ are shown in panels (e) and (f). The extended angle is only imposed on the level set function in part of the boundary on the wall.

In the next two examples, we couple the dynamics of the interface and the reinitialization of the level set function with the Navier-Stokes equation. We consider the dynamics of two-phase fluids. The flow is modeled by the incompressible Navier-Stokes equation in both phases, and the interface $\mathbf{x}_\Gamma$ between the two phases is advected by the velocity field $\mathbf{u}$. At the solid wall, we use the contact line model proposed by Ren *et al.* [35–37]. This includes the Navier slip boundary condition for $\mathbf{u}$ and a condition for the dynamic contact angle. We compute the two-phase flows and the dynamics of the interface using the level set method. The numerical scheme is similar to that used in Refs. [18,38] for 2d simulations. The level set function is reinitialized using the current method at every time step.

Example 3. We consider the spreading of a droplet on a heterogeneous solid surface. The equilibrium contact angle varies on the wall, and it is given by $\theta_Y(x,y)=\pi/2(1-1/3*\cos\varphi)$, where φ is the angle at (x,y) in the polar coordinate system with origin at $(0.75,0.75)$. The initial interface is the hemisphere $|\mathbf{x}-\mathbf{x}_4|=0.5$ where $\mathbf{x}_4=(0.75,0.75,0)$. The contact angle of the initial interface, which is 90°, differs from the local equilibrium contact angle. This discrepancy gives rise to an unbalanced Young stress at the contact line, which drives the droplet to its equilibrium state. During the relaxation, the contact line recedes inwards along the y axis, and advances outwards along the x axis. The configuration of the droplet after reaching its equilibrium state is shown in Fig. 8(d). Cross sections of the level set function and the angle extended from the contact line are also shown in the figure (panels (a)-(c) and (e)). The last panel shows the actual angle that the isosurfaces of the level set function intersect with the wall.

Example 4. In the last example, we compute the dynamics of a droplet on an inclined plane under gravitational force. Initially the droplet is given by a spherical cap with contact angle 90°. Under the gravitational force, the droplet slides downwards on the plane. First we consider the case where the two fluids have the same density and viscosity. We set the Reynolds number $Re=1$, the Capillary number $Ca=1$, and the slip length $l_s=0.1$. The equilibrium contact angle of the wall is 90°, the inclination angle of the wall is 30°, and the Bond number is 10.

https://doi.org/10.4208/cicp.210815.180316a Published online by Cambridge University Press

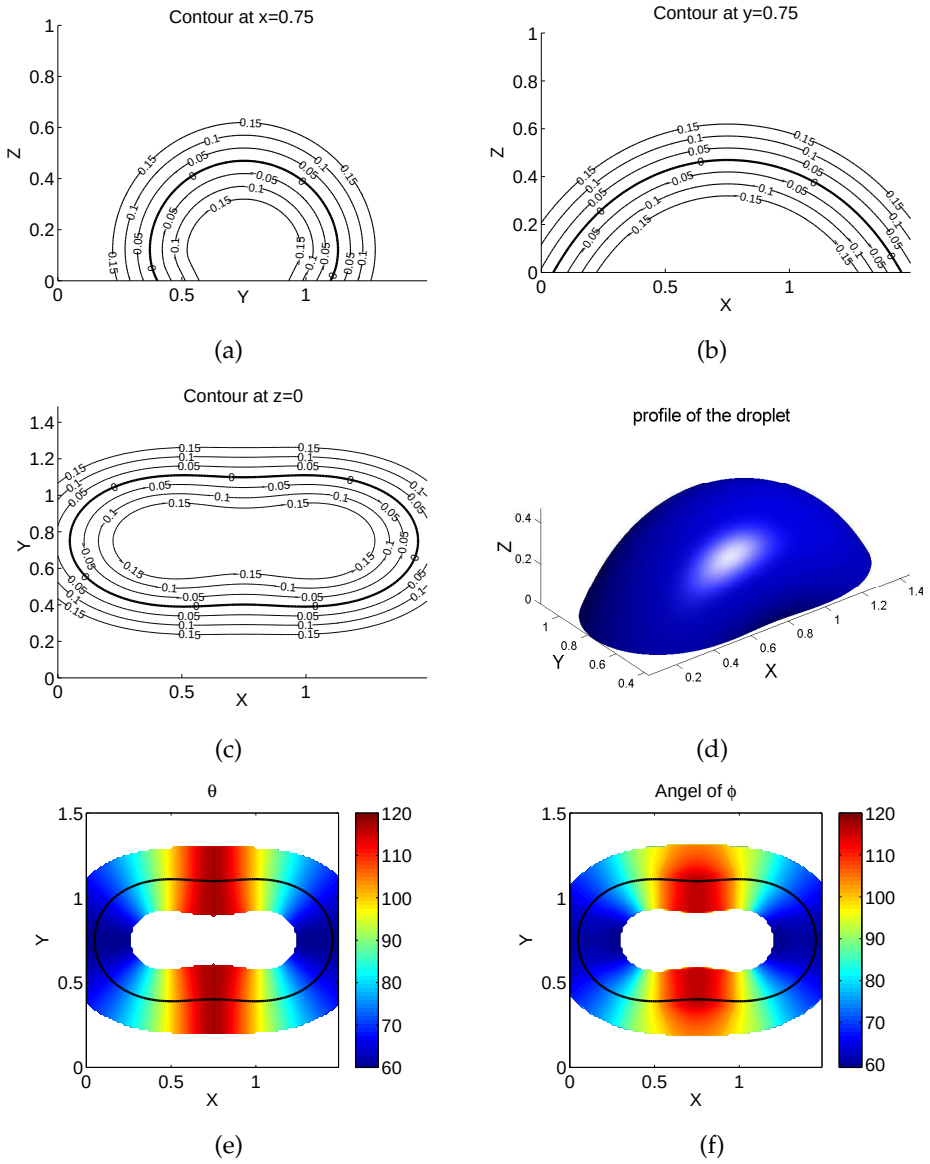


Figure 8: Numerical results for the relaxation of a droplet on a heterogeneous solid surface at $t=10$ (Example 3). (a)-(c): Contours of the level set function ϕ at and $x=0.75$, $y=0.75$ and $z=0$ respectively. (d): Configuration of the droplet. (e): The angle θ extended from the contact line. (f): The angle that the isosurfaces of ϕ make with the wall.

Under the gravitational force, the droplet deforms as it moves downwards on the plane. Snapshots of the droplet at different times are shown in Fig. 9. The angle extended from the contact line and the angle that the level set function makes with the wall at the time $t=1.75$ are also shown in the figure.

We conducted a convergence study for the numerical method using this example.

https://doi.org/10.4208/cicp.210815.180316a Published online by Cambridge University Press

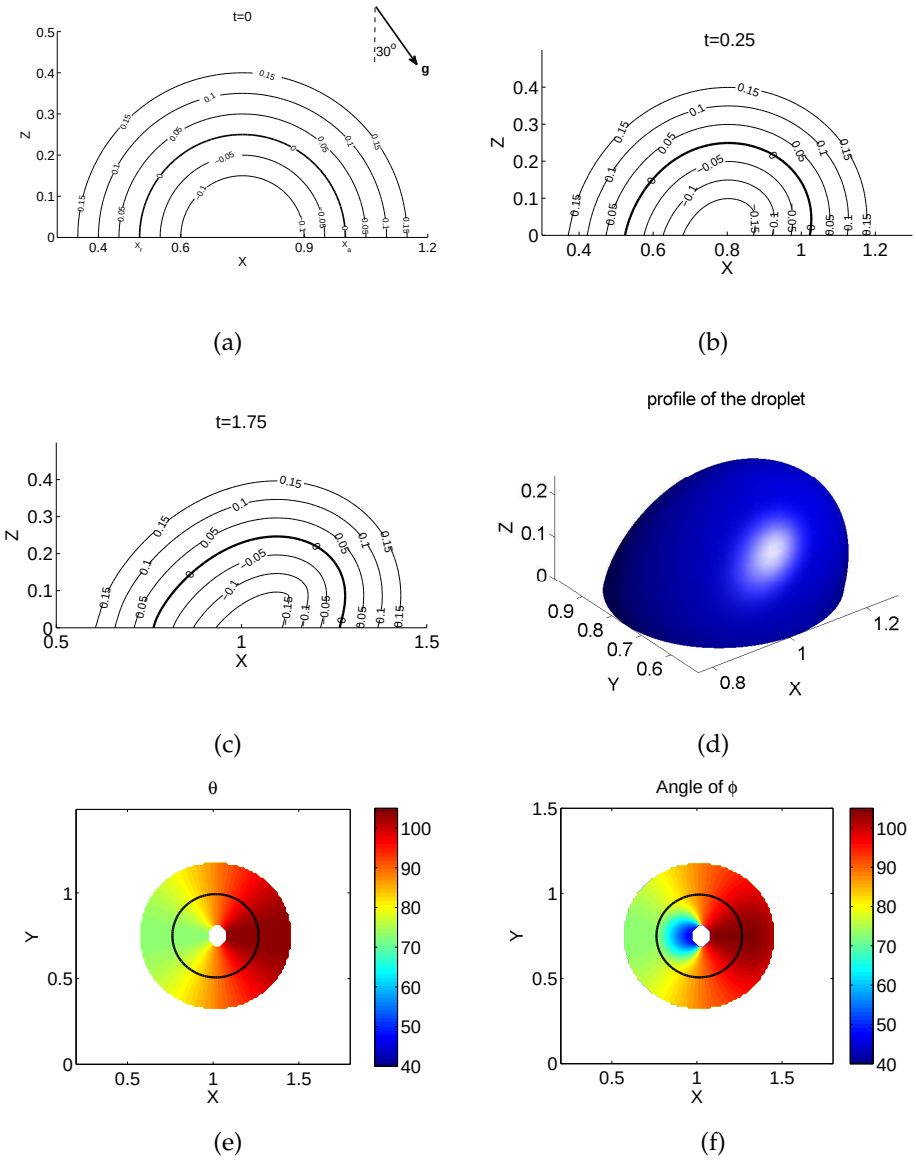


Figure 9: Dynamics of a droplet sliding on an inclined plane under gravity, where the two fluids have equal density and viscosity (Example 4). (a)-(c): Contours of the level set function at $y=0.75$ and $t=0$, 0.25, 1.75 respectively. (d): Configuration of the droplet at $t=1.75$. (e): The extended angle θ at $t=1.75$. (f): The angle that the isosurfaces of ϕ make with the wall at $t=1.75$.

In Fig. 10 we show the dynamics of the advancing contact point x_a in the front and the receding contact point x_r in the rear of the droplet computed using three different meshes with $h=1/40$, $1/80$, $1/160$ respectively. The two contact points are indicated in Fig. 9(a). Convergence can be observed from these numerical results.

Finally, we consider the case where the two fluids have different densities and vis-

https://doi.org/10.4208/cicp.210815.180316a Published online by Cambridge University Press

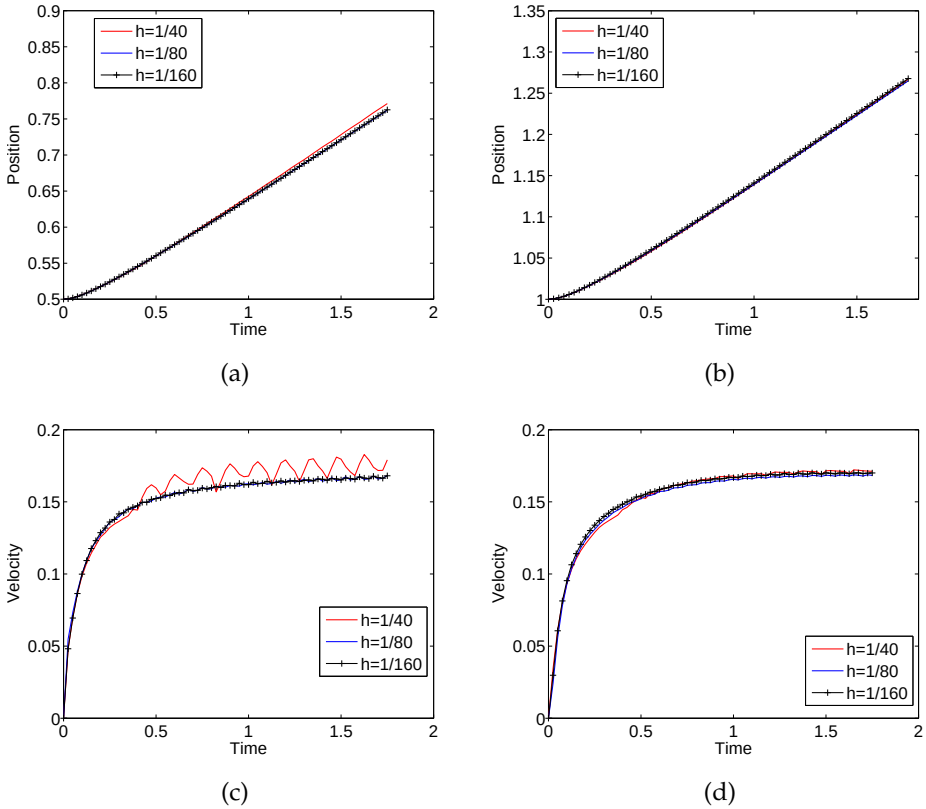


Figure 10: Convergence study for the sliding droplet on an inclined plane (Example 4). (a)-(b): Time history of the receding contact point x_r and the advancing contact point x_a computed using different meshes, respectively. (c)-(d): The receding velocity at x_r and advancing velocity at x_a, respectively.

cosities. Specifically, the density ratio of the droplet and the fluid outside is 100, and the viscosity ratio is 10. We use a pressure stabilization method to solve the Navier-Stokes equation [16, 39, 40]. Other parameters are the Reynolds number $Re=1$, the Capillary number $Ca=0.1$, the slip length $l_s=0.05$, and the Bond number $Bo=40$. The equilibrium contact angle of the wall is 90°, and the inclination angle of the wall is 60°. Numerical results computed using the mesh with $h=0.01$ are shown in Fig. 11. Initially the droplet is given by a spherical cap with contact angle 90°. In Fig. 11(a), we plot the time history of the velocity of two contact points, one in the front and the other in the rear of the droplet (x_a and x_r in panel (e)), respectively. The time history of the corresponding contact angles are shown in panel (b). It is seen that the droplet reaches the steady state at $t\approx 0.4$, after which the droplet slides downwards on the plane at a constant speed. The configuration of the droplet after reaching the steady state, the angle that the level set function makes with the wall, and the contour lines of the level set function are shown in panels (c)-(f), respectively.

https://doi.org/10.4208/cicp.210815.180316a Published online by Cambridge University Press

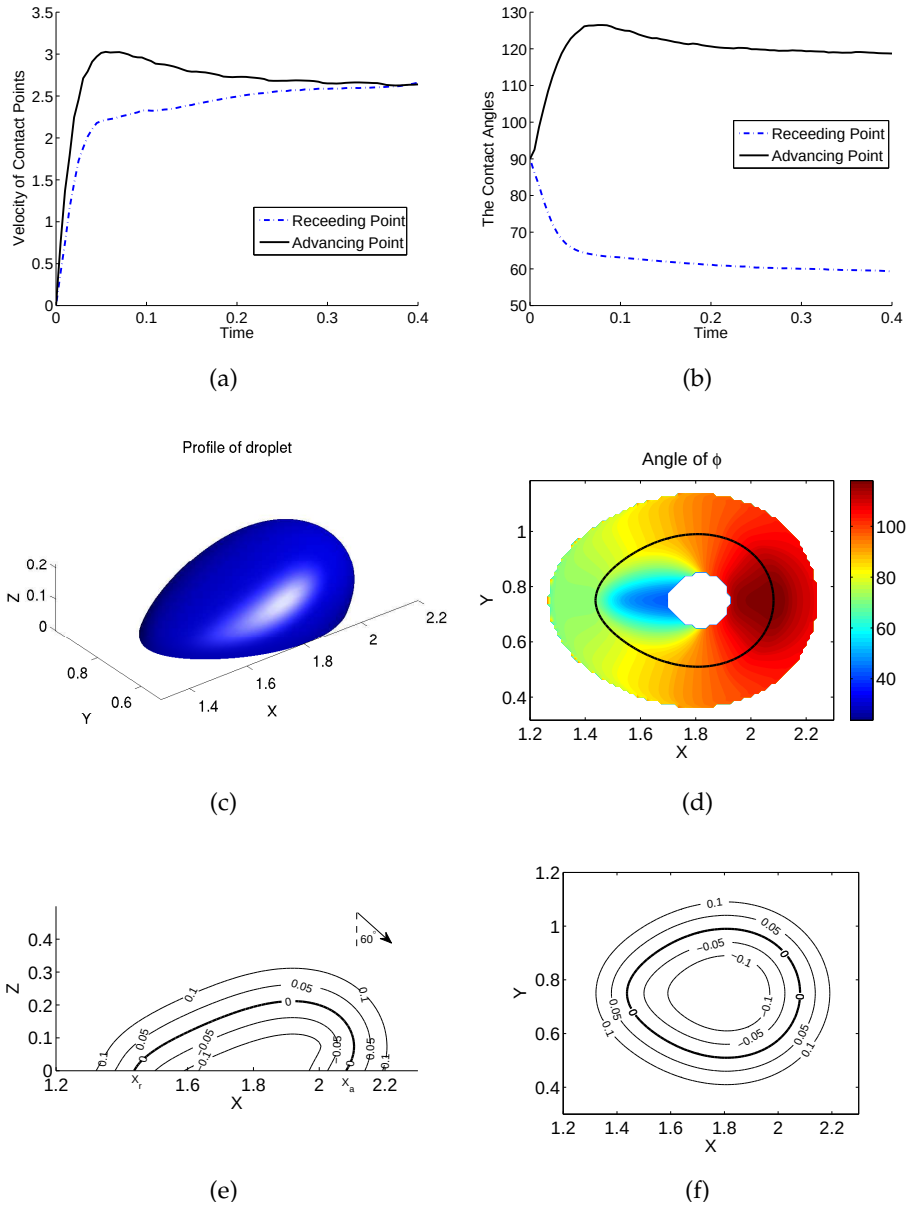


Figure 11: Dynamics of a droplet sliding on an inclined plane under gravity, where the density and viscosity ratios of the two fluids are 100 and 10, respectively (Example 4). (a): Time history of the advancing and receding velocity of the contact points x_a and x_r respectively. (b): Time history of the advancing and receding contact angle at x_a and x_r respectively. (c)-(d): An instantaneous configuration of the droplet and the angle of the corresponding level set function makes with the wall, respectively. (e)-(f): Contours of the level set function at $y=0.75$ and $z=0$, respectively.

4 Conclusions

In the simulation of multi-phase flows using the level set method, the level set function needs to be reinitialized to avoid large variations. When the fluid interface intersects

https://doi.org/10.4208/cicp.210815.180316a Published online by Cambridge University Press

with a solid wall, a moving contact line forms and the reinitialization equation, which is a transport equation, requires a boundary condition in regions where the transport velocity points from the wall into the fluids domain. In this paper, we proposed to impose the angle boundary condition on the level set function. The angle is obtained by the normal extension of the dynamic contact angle from the contact line. The reinitialization equation and the equation for the normal extension of the contact angle form a coupled system and are solved simultaneously using the 3rd order TVD Runge-Kutta method and the Godunov scheme. The numerical scheme automatically impose the boundary condition where it is needed.

The performance of the numerical method was illustrated using examples in 3d. These include examples where the level set function is computed for a given interface, and more challenging problems in which the reinitialization method is coupled with the solution of the Navier-Stokes equation. The interface is advected by the velocity field and the dynamic contact angle, which depends on the local velocity, varies along the contact line.

With this numerical method and the contact line model developed in our earlier work, we are in a position to study many interesting physical processes in multi-phase flows with moving contact lines. These applications will be left to our future work. The numerical method can be applied to many other problems involving moving contact lines as well, for example, in the simulation of dislocation dynamics in crystalline solids using the level set method [41,42].

Acknowledgments

The work was partially supported by Singapore A*STAR SERC PSF grant 1321202071, the A*STAR SERC "Complex Systems Programme" 1224504056 and the MOE Academic Research Fund Tier 1 grant R-146-000-216-112.

References

[1] E. B. Dussan, On the spreading of liquids on solid surfaces: Static and dynamic contact lines, *Annu. Rev. Fluid Mech.* 11 (1979) 371-400.
[2] P. G. de Gennes, Wetting: statics and dynamics, *Rev. Mod. Phys.* 57 (1985) 827-863.
[3] T. D. Blake, The physics of moving wetting lines, *J. Colloid Interface Sci.* 299 (2006) 1-13.
[4] D. Bonn, J. Eggers, J. Indekeu, J. Meunier, E. Rolley, Wetting and spreading, *Rev. Mod. Phys.* 81 (2009) 739-805.
[5] P.-G. de Gennes, F. Brochard-Wyart, D. Quéré, Capillarity and wetting phenomena: drops, bubbles, pearls, waves, Springer, New York (2003).
[6] V. M. Starov, M. G. Velarde, C. J. Radke, Wetting and spreading dynamics, in: Surfactant Science Series. CRC Press, Taylor & Francis Group, Boca Raton (2007).
[7] Y. D. Shikhmurzaev, Capillary flows with forming interfaces, Chapman & Hall/CRC, Boca Raton (2008).

https://doi.org/10.4208/cicp.210815.180316a Published online by Cambridge University Press

[8] S. Afkhami, M. Bussmann, Height functions for applying contact angles to 3D VOF simulations, *Int. J. Numer. Methods Fluids* 61 (2008) 827-847.
[9] S. Afkhami, S. Zaleski, M. Bussmann, A mesh-dependent model for applying dynamic contact angles to VOF simulations, *J. Comput. Phys.* 228 (2009) 5370-5389.
[10] M. Renardy, Y. Renardy, J. Li, Numerical simulation of moving contact line problems using a volume-of-fluid method, *J. Comput. Phys.* 171 (2001) 243-263.
[11] H. Huang, D. Liang, B. Wetton, Computation of a moving drop/bubble on a solid surface using a front-tracking method, *Commun. Math. Sci.* 2 (2004) 535-552.
[12] M.-C. Lai, Y.-H. Tseng, H. Huang, Numerical simulation of moving contact lines with surfactant by immersed boundary method, *Commun. Comput. Phys.* 8 (2010) 735-757.
[13] T. Qian, X.-P. Wang, P. Sheng, Molecular scale contact line hydrodynamics of immiscible flows, *Phys. Rev. E* 68 (2003) 016306.
[14] T. Qian, X.-P. Wang, P. Sheng, Molecular hydrodynamics of the moving contact line in two-phase immiscible flows, *Commun. Comput. Phys.* 1 (2006) 1-52.
[15] P. Yue, C. Zhou, J. J. Feng, Sharp-interface limit of the Cahn-Hilliard model for moving contact lines, *J. Fluid Mech.* 645 (2010) 279-294.
[16] M. Gao, X.-P. Wang, An efficient scheme for a phase field model for the moving contact line problem with variable density and viscosity, *J. Comput. Phys.* 272 (2014) 704-718.
[17] P. D. M. Spelt, A level-set approach for simulations of flows with multiple moving contact lines with hysteresis, *J. Comput. Phys.* 207 (2005) 389-404.
[18] J.-J. Xu, W. Ren, A level-set method for two-phase flows with moving contact line and insoluble surfactant, *J. Comput. Phys.* 263 (2014) 71-90.
[19] K. Yokoi, D. Vadillo, J. Hinch, I. Hutchings, Numerical studies of the influence of the dynamic contact angle on a droplet impacting on a dry surface, *Phys. Fluids* 21 (2009) 072102.
[20] Z. Li, M.-C. Lai, G. He, H. Zhao, An augmented method for free boundary problems with moving contact lines, *Comput. Fluids* 39 (2010) 1033-1040.
[21] Y. Sui, H. Ding, P. D. M. Spelt, Numerical simulations of flows with moving contact lines, *Annu. Rev. Fluid Mech.* 46 (2014) 97-119.
[22] S. Osher, R. Fedkiw, Level set methods and dynamic implicit surfaces, Applied mathematical science, Springer, New York (2003).
[23] G. Della Rocca, G. Blanquart, Level set reinitialization at a contact line, *J. Comput. Phys.* 265 (2014) 34-49.
[24] M. Sussman, S. Uto, A computational study of the spreading of oil underneath a sheet of ice, *CAM Report*, 98-32 (1998).
[25] M. Sussman, An adaptive mesh algorithm for free surface flows in general geometries, In: A. Vande Wouwer, Ph. Saucez, W.E. Schiesser, Adaptive Method of lines. Chapman & Hall/CRC Press (2001) 207-231.
[26] M. Griebel, M. Klitz, Simulation of droplet impact with dynamic contact angle boundary condition, Singular Phenomena and Scaling in Mathematical Models, Springer, Switzerland, 2014.
[27] J.-J. Xu, Z. Li, J. Lowengrub, H. Zhao, A level set method for solving interfacial flows with surfactant, *J. Comput. Phys.* 212 (2006) 590-616.
[28] J.-J. Xu, H. Zhao, An Eulerian formulation for solving partial differential equations along a moving interface, *J. Sci. Comput.* 19 (2003) 573-594.
[29] H. Zhao, S. Osher, R. Fedkiw, A variational level set approach to multiphase motion, *J. Comput. Phys.* 127 (1996) 179-195.
[30] D. Hartmann, M. Meinke, W. Schröder, The constrained reinitialization equation for level

https://doi.org/10.4208/cicp.210815.180316a Published online by Cambridge University Press

set methods, *J. Comput. Phys.* 229 (2010) 1514-1535.
[31] G.-S. Jiang, D. P. Peng, Weighted ENO schemes for Hamilton-Jacobi equations, *SIAM J. Sci. Comput.* 21 (2000) 2126-2143.
[32] D. Adalsteinsson, J. A. Sethian, A fast level set method for propagating interfaces, *J. Comput. Phys.* 118 (1995) 269-277.
[33] D. P. Peng, B. Merriman, S. Osher, H. Zhao, M. Kang, A pde-based fast local level set method, *J. Comput. Phys.* 155 (1999) 410-438.
[34] C.-W. Shu, Total-variation-diminishing time discretizations, *SIAM J. Sci. and Stat. Comput.* 9 (1988) 1073-1084.
[35] W. Ren, W. E, Boundary conditions for the moving contact line problem, *Phys. Fluids* 19 (2007) 022101.
[36] W. Ren, D. Hu, W. E, Continuum models for the contact line problem, *Phys. Fluids* 22 (2010) 102103.
[37] W. Ren, W. E, Derivation of continuum models for the moving contact line problem based on thermodynamic principles, *Commun. Math. Sci.* 9 (2011) 597-606.
[38] W. Ren, W. E, Contact line dynamics on heterogeneous surfaces, *Phys. Fluids* 23 (2011) 072103.
[39] J.-L. Guermond, A. Salgado, A splitting method for incompressible flows with variable density based on a pressure Poisson equation, *J. Comput. Phys.* 228 (2009) 2834-2846.
[40] J. Shen, X. Yang, A phase-field model and its numerical approximation for two-phase incompressible flows with different densities and viscosities, *SIAM, J. Sci. Comput.* 32 (3) (2010) 1159-1179.
[41] Y. Xiang, L.-T. Cheng, D. J. Srolovitz, W. E, A level set method for dislocation dynamics, *Acta Mater.* 51 (2003) 5499-5518.
[42] A. Y. Zhu, C. M. Jin, D. G. Zhao, Y. Xiang, J. F. Huang, A numerical scheme for generalized Peierls-Nabarro model of dislocations based on the fast multipole method and iterative grid redistribution, *Commun. Comput. Phys.* 12 (2012) 226-246.

https://doi.org/10.4208/cicp.210815.180316a Published online by Cambridge University Press